RSC Advances

PAPER

View Article Online
View Journal | View Issue

Check for updates

Cite this: *RSC Adv.*, 2020, **10**, 6497

Amine decorated polystyrene nanobeads incorporating π-conjugated OPV chromophore for picric acid sensing in water†

Sarabjot Kaur Makkad *[ab]

Received 25th November 2019
Accepted 29th January 2020

DOI: 10.1039/c9ra09852f

rsc.li/rsc-advances

A solution as well as solid state based sensor has been developed for selective detection of picric acid (PA) in water. Oligo (*p*-phenylenevinylene) (OPV) incorporated polystyrene nanobeads (PS-OPV-NH_2) having an average size of 180 nm have been synthesized through miniemulsion polymerization. Amine ($-NH_2$) functionalization was performed on the nanobead surface to enhance the efficiency of the sensor among a library of other nitro-organics and library of cations and anions.

Introduction

Sensitive and selective sensing of nitroexplosives is of immense importance for security reasons and environmental protection.[1]Unlike the rest, picric acid (PA) is widely used in dye and drug industries, pesticide manufacturing *etc*.[2] This makes it easier to enter the environment and pollute soil and natural water resources, causing several concerns.[3–5] Multiple fluorescence based sensors like quantum dots (QD),[6] polymers,[7]upconverting nanoparticles (UCNP),[8] metal–organic frameworks (MOF),[9] small molecules[10] *etc.* are available for detection of PA. One such example of a MOF based sensor has been reported by Shi *et al.*[11] for detection of PA in dimethyl acetamide. Likewise Sang *et al.*[12] and Venkatramaiah *et al.*[10] reported a covalent organic framework and small molecule based PA sensor in methanol and ethanol respectively. Most of these sensors are tested to detect PA from organic solvents, and often suffer from crucial limitations such as less selectivity,[10,13–15] poor water dispersibility, aggregation induced emission quenching in aqueous medium, *etc*.[10–16] Additional factors such as use of toxic metals, temperature/pH dependent emission in the case of MOF, UCNP and QD, instability in water limits their practical applicability.[16–18] This leads to a continuous stretch in search for a fluorescence based sensor for picric acid to check and prevent any possible harm in terms of environmental pollution and detecting buried explosives.

In this context, polymer based sensors always hold superiority in terms of high quantum efficiency, tunable emission, *etc*. However, in such sensors, lack of specific binding site for the interaction with analytes[19–21] along with multistep tedious synthesis,[19,21,22] sometime limits their application. Additionally, interference of other nitro-organics[22–25] or some heavy metal ions[20,25,26] *e.g.* Cu(II), Ni(II), Fe(III), Zn(II) (that are present in water) are significant and hence their removal is required prior to the sensing test for PA.[26]

In an attempt to overcome these limitations without compromising the selectivity and sensitivity, we are presenting two approaches, covalent stitching of fluorophore and surface functionalization of the nanobeads. Herein, we have prepared amine ($-NH_2$) functionalized polystyrene (PS) based sensor for visual detection of PA using green and environmentally benign miniemulsion polymerization method (Scheme 1). Oligo (*p*-phenylenevinylene) (OPV) was covalently stitched[27] to the polymer backbone to prevent any dye leaching during application

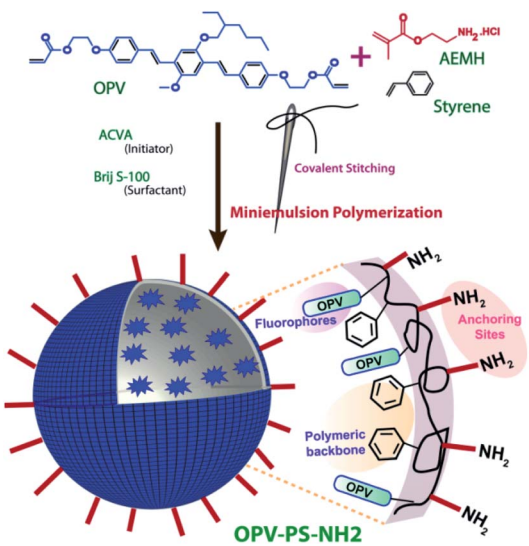

Scheme 1 Schematics for synthesis of amine decorated polystyrene nanobeads *via* miniemulsion polymerization.

[a]*Govt. Autonomous NPG College of Science, Raipur, India. E-mail: sarabjot31@gmail.com*

[b]*CSIR-National Chemical Laboratory, Pune, India*

† Electronic supplementary information (ESI) available. See DOI: 10.1039/c9ra09852f

Open Access Article. Published on 11 February 2020. Downloaded on 2/8/2026 2:06:00 AM.
This article is licensed under a Creative Commons Attribution-NonCommercial 3.0 Unported Licence.

Open Access Article. Published on 11 February 2020. Downloaded on 2/8/2026 2:06:00 AM.
This article is licensed under a Creative Commons Attribution-NonCommercial 3.0 Unported Licence.

cycles. Amine functionalization on the surface of the nanobeads was performed with the view to provide specific binding sites for the analytes and to improve its selectivity by boosting analyte–sensor interaction. Furthermore, interference from almost 16 cations [including Fe(III), Zn(II), Ni(II), Cu(II) *etc.*] that are commonly present in water were checked to test their effect on sensor performance. Device applicability and reusability of sensor was checked further by casting free standing film from polymer. Thus efficient, prompt and highly selective on-site sensing of PA was achieved in pure aqueous medium.

Experimental

Materials

4,4′-Azobis(4-cyanovaleric acid) (ACVA), Brij S-100, potassium persulfate (KPS), aminoethyl methacrylate hydrochloride (AEMH) were purchased from Aldrich and *n*-hexadecane (HD) from Alfa Aesar and were used without any further purification. Styrene was purchased from Aldrich and was purified as per the standard protocol. All the analytes used for sensing studies including nitro-organics and inorganic salts were purchased from commercially available sources and used as received. Solvents and other reagents were purchased from local suppliers and further purified using standard procedures. Deionized water was used throughout the studies. OPV dye with double bond at both termini for covalent attachment to the polymer backbone was synthesized based on our previous report.[27]

Measurements

The details of instrumental techniques used for characterization of polymer such as DLS (for size and zeta potential), GPC, TEM, sonicator, NMR, absorption and fluorescence spectrophotometer are same as described in our earlier report.[27]

The pH dependent studies were carried out using 100 μg of polymer that was taken in various mentioned pH (3 mL) followed by recording its emission spectra. For temperature dependent studies, 100 μg of the polymer in 3 mL deionized water was taken and emission spectra was recorded using Peltier sample compartment with a thermoelectric temperature controller and autotone PID. The temperature was set manually with a tolerance range of 0.5 °C and an equilibration time of 10 minute before each reading. The temperature was fixed. All the emission experiments were performed in deionized water and slit width of 1 nm and "S1c/R1" mode was maintained throughout the studies. For TEM, polymer sample in water was drop casted into carbon coated copper grid and solvent was allowed to dry at room temperature.

Preparation of fluorescent polystyrene nanoparticles

Amine functionalized OPV incorporated polystyrene nanobeads was prepared as per the reported article.[28] For the same, the organic phase containing 1 g of styrene, 30 mg OPV and 48 mg of hexadecane was dropwise added to an aqueous phase (4 mL) containing 100 mg of AEMH, 16 mg of ACVA and 33 mg of Brij S-100. This mixture was then pre-emulsified for an hour at room temperature. The obtained emulsion was then sonicated for another 20 min under an ice-cooled bath. Finally, the polymerization was carried out at 70 °C for 20 h with a constant stirring at 750 rpm. The obtained latex was dialyzed using a dialysis membrane (molecular weight cutoff = 6 kDa) against deionised water for 3 days, with changing water every six hours. The percentage solid content of the polymer was calculated using standard equation.[27] The solid content value of PS-OPV-NH_2 is given in Table S1.†

Estimation for dye incorporation into nanobeads

Dye Loading Content (DLC) and Dye Loading Efficiency (DLE) was calculated by taking 1 mg mL^{-1} of the polymer in tetrahydrofuran (THF) and its absorbance was measured subsequently at its absorption maxima at 365 nm. The amount of dye incorporated into polymer backbone was calculated based on its absorption coefficient (40 360 L mol^{-1} cm^{-1}) in THF. Further its DLC and DLE values were calculated using standard equations.[27]

Sample preparation and study of chemical sensing

For sensing studies of nitro-organics in water, 100 μg of PS-OPV-NH_2 was dispersed into 3 mL of deionized water. And to the same was added fixed concentration (10^{-4} M) of various analytes listed in Scheme S1.† The solution was then subjected to thorough mixing followed by immediate recording of the emission spectra. All the experiments were repeated thrice to avoid any discrepancy and average of the three values was plotted as bar graph along with their standard error. For sensing of PA in water, various concentration of PA was added to the fixed volume of polymer mentioned above and its emission as well as excitation spectra were recorded. Interference from various anions and cations in water was checked using same concentration (10^{-4} M) for each of the analytes. For free standing film, 20 mg of polymer was dissolved in 1 mL THF and poured into a Petridish. After evaporation of the solvent, the film (thickness 0.04 ± 0.02 mm) was peeled off. The emission spectra were recorded immediately after dipping into the PA solution in water.

The polymer sample was excited at $\lambda_{excitation} = 390$ nm (OPV) and subsequently its emission spectra was collected in the range of 400–700 nm.

The equations of percentage quenching (eqn (1))[9] and Stern Volmer (eqn (2))[9] are given below:

$$\%\ \text{Quenching} = \frac{I_0 - I}{I_0} \times 100 \quad (1)$$

$$\frac{I_0}{I} = K[\text{Q}] + 1 \quad (2)$$

where I_0 and I are the emission intensities at its emission maxima (446 nm) before and after the exposure to the analyte, respectively. All the percentage quenching values are tabulated in Tables S3–S5.†

 This journal is © The Royal Society of Chemistry 2020

Open Access Article. Published on 11 February 2020. Downloaded on 2/8/2026 2:06:00 AM.
This article is licensed under a Creative Commons Attribution-NonCommercial 3.0 Unported Licence.

Results and discussion

π-Conjugated OPV based dye was first synthesized and characterized as per our previously reported procedures.[27] The dye was then covalently incorporated into polystyrene backbone through miniemulsion co-polymerization, using non-ionic Brij S-100 as surfactant and 4,4′-azobis(4-cyanovaleric acid) as initiator. Aminoethyl methacrylate hydrochloride was used as functional monomer to functionalize the surface of the resulting nanobeads (PS-OPV-NH_2) with $-NH_2$ group. The surface charge was confirmed by a net elevated positive zeta potential of +36.6 mV, indicating presence of $-NH_2$ groups on the surface (Table S1†). FTIR analysis further confirmed the presence of $-NH_2$ group, from the presence of characteristic peaks (Fig. S1†). Broad peak centered at 3408 cm^{-1} accounted for N–H stretching while the in-plane bending resulted in a sharp peak at 1604 cm^{-1}. Another broad peak at 1100 cm^{-1} accounted for C–N stretching. The relative molecular weight was determined by gel permeation chromatography (GPC) in chloroform ($CHCl_3$). It was found to possess high molecular weight in the range of 151 kDa (M_w) with PDI value of 2.6 and the values are tabulated in Table S1.† The size of the nanobeads, as observed from particle size analysis with dynamic light scattering was 182 nm with PDI value of 0.08, signifying uniform size distribution as obtained by miniemulsion polymerization approach (Fig. S2 and Table S2†). TEM imaging further confirmed spherical morphology of the nanobeads (Fig. S3†).

Low incorporation of the OPV dye into polymer backbone prevented the detection of its characteristic signals by NMR spectroscopy. However, its presence could easily be identified and quantified from the absorption spectrum recorded in THF (Fig. S4†). The nanobeads showed an absorption maximum at 365 nm,[27] corresponding to the incorporated OPV moieties, with a blue shift of 30 nm compared to pristine dye. The amount of dye incorporated into polymer backbone has been quantified based on its molar absorptivity value (40 360 L mol^{-1} cm^{-1}, THF), following the standard equations of dye loading content (DLC) and dye loading efficiency (DLE) calculation. Its DLC value was found to be 1.6% while its DLE was 53.6% (Table S2†), showing an efficient insertion of the OPV dyes into the polystyrene core.

Fig. S5† displays the emission and excitation spectra of PS-OPV-NH_2 in water. The excitation wavelength for emission was 390 nm while the excitation spectrum was collected at 445 nm. Polymer showed bright blue emission in water under UV lamp which was further confirmed by its CIE co-ordinate diagram with CIE co-ordinate value of (0.15, 0.14) (Fig. S6†). Its excitation spectra distinctly exhibited two vibrational bands at 345 nm and 365 nm. Further, the effect of pH and temperature variation on the emission properties of polymer was studied. The results clearly showed that the emission remained unaffected for a wide range of temperature and pH. This highlighted the advantage of polystyrene nanobeads, where a constant emission was possible under different conditions, unlike QDs and UCNPs which might hamper the sensing ability of sensor (Fig. S7 and S8†).

The high emissive nature of PS-OPV-NH_2 in water, good water dispersibility, in addition to the excellent thermal[27] and photostability, makes it desirable candidate to be used for fluorescence based chemo sensor in water. During our previous investigation, we have seen that electron-rich nature of OPV fluorophore helps it to interact with highly volatile electron-deficient analyte vapors.[28] This prompted us to explore the usability of OPV containing fluorescent nanoparticles for detection of nitroexplosives in contaminated water. Furthermore, we have also functionalized the nanoparticle surface with $-NH_2$ groups to increase the interaction between OPV dye and the incoming nitroexplosives, thereby increasing the overall sensing performance.

To check the selectivity of sensor toward picric acid (PA) among other organic analytes, fluorescence titration experiments were conducted by addition of fixed concentration of various analytes (10^{-4} M) listed in Scheme S1† into the water dispersion of PS-OPV-NH_2 (details of experiment are provided in Experimental section). Fig. 1(A and B) compares the effect of various analytes on the % quenching of sensor. The results clearly demonstrated the selectivity of sensor towards nitrophenols (PA, 2,4-DNP, 2-NP) while no remarkable change in fluorescence intensity was observed on the addition of other analytes. Fig. 1C shows the gradual increase in % quenching on increasing concentration of PA with instant fluorescence quenching of ~29% at 1×10^{-5} M concentration which reached ~92% at 1×10^{-4} M concentration. The inset in Fig. 1C shows the marked disappearance of the blue emission from polymer on addition of PA to it, upon observation under a UV lamp. Fig. 1D shows the simultaneous decrease in the excitation spectra on addition of PA which further supports the decrease in emission intensity of polymer with the increase in the concentration of PA. This showed rapid and prompt sensing of PA useful for on-site detection of explosives.

To analyse the reason behind the selective sensing of PA among the library of other nitro-organics and its mechanism, the fluorescence quenching was further studied using Stern–Volmer equation.[21] Fig. 1E shows the correlation between fluorescence intensity of PS-OPV-NH_2 and PA concentration. The linear fitting of plot (Fig. S9†) displayed two clear linear range of I_0/I *vs.* PA concentration which ranged from 0 to 30 μM (R^2 = 0.982) and 40 to 70 μM (R^2 = 0.998). The limit of detection was calculated based on signal to noise ratio of 3 and it was estimated to be 58 nM which indicated appreciably high sensitivity of sensor toward PA.[21]

The non-linearity in the *S–V* plot indicated amplified quenching thereby suggesting the involvement of more than one quenching mechanism which may include (a) ground state complex formation between polymer and PA (b) energy transfer (c) inner filter effect (IFE) (d) photoinduced electron transfer (PET) from PS-OPV-NH_2 to PA. To get a deeper understanding, the absorption spectra of polymer with varying concentration of PA were recorded (Fig. S10†) and no obvious shift or appearance of new peak in the absorption spectra was observed in presence of PA. This ruled out the possibility of quenching by ground state complex formation between PA and polymer. Furthermore, Fig. S11† shows evident spectral overlap between

Open Access Article. Published on 11 February 2020. Downloaded on 2/8/2026 2:06:00 AM.
This article is licensed under a Creative Commons Attribution-NonCommercial 3.0 Unported Licence.

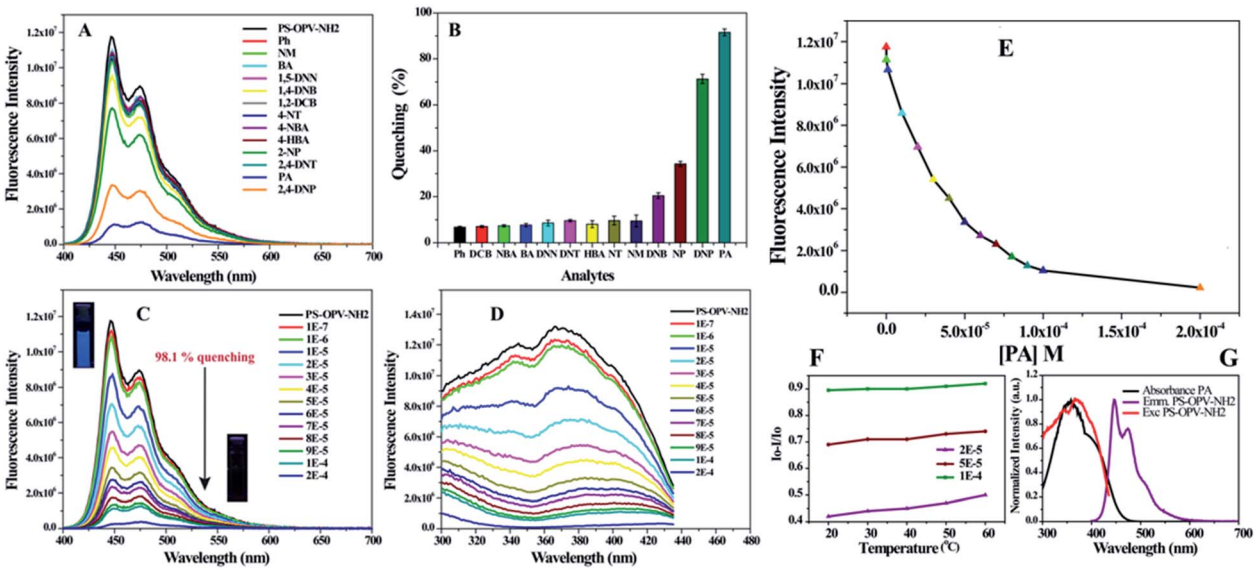

Fig. 1 (A) Emission spectra of PS-OPV-NH_2 and (B) quenching percentage upon addition of different nitro-organic compounds (1×10^{-4} M) in water. (C) Emission and (D) excitation spectra of PS-OPV-NH_2 collected after addition of varying concentration of PA (1×10^{-7} to 2×10^{-4} M). Emission and excitation spectra were collected at $\lambda_{ex} = 390$ nm and $\lambda_{em} = 445$ nm respectively. (E) Plot of changes in fluorescence intensity of PS-OPV-NH_2 *vs.* conc. of PA. (F) Temperature dependent quenching of polymer emission after PA addition. (G) Spectral overlap of excitation/emission spectra of PS-OPV-NH_2 with that of absorption spectra of PA.

emission spectra of polymer and absorption spectra of nitrophenols while inefficient overlap was observed for the rest of the analytes. This result supported the involvement of long range energy transfer in the quenching process. Also, emission quenching efficiency of PA recorded at different temperature confirmed the nature of quenching to be static type. Fig. 1F showed no appreciable change in quenching of polymer after PA addition (2×10^{-5} to 1×10^{-4} M) as a function of temperature (20 °C to 60 °C); confirming static quenching which further verifies energy transfer from polymer to PA.[21,29] Additionally, complete overlap of the absorption spectra of PA (λ_{max} = 360 nm) with excitation spectra of OPV-PS-NH_2 (λ_{max} = 365 nm) also indicated possibility of inner filter effect which reduces the fluorescence intensity of fluorophore due to competitive absorption by PA resulting in non-linearity between concentration of analyte and observed fluorescence intensity of fluorophore (Fig. 1G). But it is to be noted that spectral overlap between emission/excitation spectra of polymer to that of absorption spectra of PA or 2,4-DNP was almost same (Fig. S11†), however % quenching by these compounds followed the order: PA > 2,4-DNP > 2-NP. This can be attributed to PET *via* acid base interaction since they all contained one hydroxyl (–OH) group with varying nitro group that governed their acidity. To further verify the role of functional group in sensing, effect of compounds with only –OH group (Ph, 4-HBA) or only –NO_2 group (1,4-NBA, 4-NT, 2,4-DNT, 1,2-DCB, 1,5-DNN) on % quenching of polymer was checked. As shown in Fig. 1(A and B) no obvious effect on the emission spectra of polymer was observed by their addition which reassured the requirement of both –OH as well as –NO_2 group in the sensing mechanism.

Hence on the basis of above discussion, it is quite clear that outstanding selectivity and sensitivity of polymer toward PA sensing in water is due to the combined effect of three mechanisms namely, energy transfer, PET and IFE (Fig. 2A).

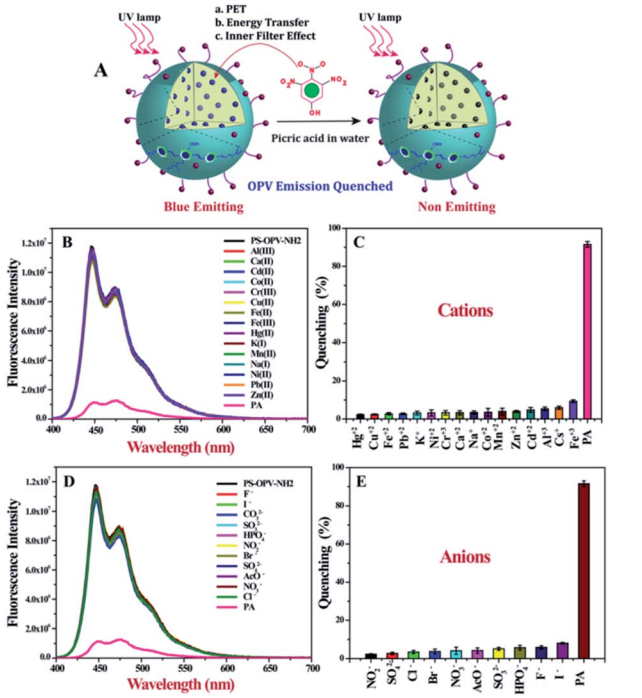

Fig. 2 (A) Schematics for the mechanism of quenching of OPV emission by PA in water. (B) Emission spectra of PS-OPV-NH_2. (C) Its comparative quenching percentage upon addition of different cations *vs.* PA (1×10^{-4} M) in water. (D) Emission spectra of PS-OPV-NH_2 and (E) its comparative quenching percentage upon addition of different anions *vs.* PA (1×10^{-4} M) in water.

 This journal is © The Royal Society of Chemistry 2020

Open Access Article. Published on 11 February 2020. Downloaded on 2/8/2026 2:06:00 AM.
This article is licensed under a Creative Commons Attribution-NonCommercial 3.0 Unported Licence.

As sensing studies was performed in aqueous medium, it was crucial to check for possible interference from cations and anions that might be present in the contaminated water sample. Almost 16 different cations were chosen including both hard and soft metal ions and as shown in Fig. 2B and C none of the metal ions exhibited any obvious quenching of the emission spectra of PS-OPV-NH_2 unlike other sensors where hard metal ions have to be first complexed with EDTA before carrying out PA sensing. This clearly establishes an advantage in terms of ready to use nature of the sensor.

Similarly a library of anions was also checked (Fig. 2C and D) and none were found to affect the emission intensity of polymer. We also explored effect of ionic strength on the sensing efficiency of PA. To demonstrate the same the emission spectra of polymer before and after the addition of 1 M NaCl was collected and no change in its emission intensity was observed (Fig. S12†). Also fluorescence quenching efficiency of PA remained similar even after the addition of 1 M NaCl indicating that sensor had the capability to withstand the complex environment and could be used for PA sensing even in sea water.

Scope of PS-OPV-NH_2 for real time device based application was tested using a free-standing membrane (λ_{max} = 477 nm), prepared from evaporating the THF solution of the polymer on a glass surface. When the film was dipped in PA contaminated water (PA conc. of 2×10^{-4} M) for 1 min, an instant drop in the emission was observed, measuring 53% quenching of the original intensity (Fig. S13†). This demonstrated the high potential of OPV-PS-NH_2 towards device based application for detection of PA from aqueous medium, in the form of self-standing film.

Conclusion

We have developed both solution and solid state PS sensor for the selective sensing of PA in aqueous medium. The surface of nanobeads was decorated with $-NH_2$ group with the aim to enhance analyte–sensor interaction thereby improving selectivity of sensor. The outstanding selectivity of the sensor among the library of other nitro-organics was attributed to combined effect of energy transfer, inner filter effect and electron transfer. The concentration of PA as low as 58 nM in 100% water could be effectively detected by the sensor. Additionally, no interference from large number of cations and anions was observed making the sensor highly efficient for real water analysis. Also, its emission remained independent of external triggers; making it applicable over wide range of temperature and pH. For device based application free standing film was made. Thus rapid, efficient, sensitive sensor was developed for the selective detection of PA in water.

Conflicts of interest

There are no conflicts to declare.

Acknowledgements

Author thanks CSIR for Shyama Prasad Mukherjee (SPM) fellowship. I would also like to acknowledge Dr Asha S. K. for providing and helping me with the lab facilities and her invaluable inputs in CSIR-NCL, Pune.

Notes and references

1 Y. Salinas, R. Martínez-Máñez, M. D. Marcos, F. Sancenón, A. M. Costero, M. Parra and S. Gil, *Chem. Soc. Rev.*, 2012, **41**, 1261–1296.
2 S. S. Nagarkar, A. V. Desai and S. K. Ghosh, *Chem. Commun.*, 2014, **50**, 8915–8918.
3 A. H. Malik, S. Hussain, A. Kalita and P. K. Iyer, *ACS Appl. Mater. Interfaces*, 2015, **7**, 26968–26976.
4 S. J. Toal and W. C. Trogler, *J. Mater. Chem.*, 2006, **16**, 2871–2883.
5 J. Ye, L. Zhao, R. F. Bogale, Y. Gao, X. Wang, X. Qian, S. Guo, J. Zhao and G. Ning, *Chem.–Eur. J.*, 2015, **21**, 2029–2037.
6 M. Bai, S. Huang, S. Xu, G. Hu and L. Wang, *Anal. Chem.*, 2015, **87**, 2383–2388.
7 A. S. Tanwar, S. Hussain, A. H. Malik, M. A. Afroz and P. K. Iyer, *ACS Sens.*, 2016, **1**, 1070–1077.
8 Y. Ma, S. Huang, M. Deng and L. Wang, *ACS Appl. Mater. Interfaces*, 2014, **6**, 7790–7796.
9 S. Sanda, S. Parshamoni, S. Biswas and S. Konar, *Chem. Commun.*, 2015, **51**, 6576–6579.
10 N. Venkatramaiah, S. Kumar and S. Patil, *Chem. Commun.*, 2012, **48**, 5007–5009.
11 Z.-Q. Shi, Z.-J. Guo and H.-G. Zheng, *Chem. Commun.*, 2015, **51**, 8300–8303.
12 N. Sang, C. Zhan and D. Cao, *J. Mater. Chem. A*, 2015, **3**, 92–96.
13 B. Gole, A. K. Bar and P. S. Mukherjee, *Chem.–Eur. J.*, 2014, **20**, 13321–13336.
14 B. Roy, A. K. Bar, B. Gole and P. S. Mukherjee, *J. Org. Chem.*, 2013, **78**, 1306–1310.
15 V. Bhalla, A. Gupta, M. Kumar, D. S. S. Rao and S. K. Prasad, *ACS Appl. Mater. Interfaces*, 2013, **5**, 672–679.
16 S. S. Nagarkar, B. Joarder, A. K. Chaudhari, S. Mukherjee and S. K. Ghosh, *Angew. Chem., Int. Ed.*, 2013, **52**, 2881–2885.
17 O. S. Wolfbeis, *Chem. Soc. Rev.*, 2015, **44**, 4743–4768.
18 A. Reisch and S. Klymchenko Andrey, *Small*, 2016, **12**, 1968–1992.
19 Y. Liu, M. Gao, J. W. Y. Lam, R. Hu and B. Z. Tang, *Macromolecules*, 2014, **47**, 4908–4919.
20 S. Hussain, A. H. Malik, M. A. Afroz and P. K. Iyer, *Chem. Commun.*, 2015, **51**, 7207–7210.
21 A. Qin, J. W. Y. Lam, L. Tang, C. K. W. Jim, H. Zhao, J. Sun and B. Z. Tang, *Macromolecules*, 2009, **42**, 1421–1424.
22 T. Wang, N. Zhang, R. Bai and Y. Bao, *J. Mater. Chem. C*, 2018, **6**, 266–270.
23 J. Wang, J. Mei, W. Yuan, P. Lu, A. Qin, J. Sun, Y. Ma and B. Z. Tang, *J. Mater. Chem.*, 2011, **21**, 4056–4059.
24 H. Zhou, J. Li, M. H. Chua, H. Yan, B. Z. Tang and J. Xu, *Polym. Chem.*, 2014, **5**, 5628–5637.
25 W. Z. Yuan, H. Zhao, X. Y. Shen, F. Mahtab, J. W. Y. Lam, J. Z. Sun and B. Z. Tang, *Macromolecules*, 2009, **42**, 9400–9411.

Open Access Article. Published on 11 February 2020. Downloaded on 2/8/2026 2:06:00 AM.
This article is licensed under a Creative Commons Attribution-NonCommercial 3.0 Unported Licence.

26 S. G. Liu, D. Luo, N. Li, W. Zhang, J. L. Lei, N. B. Li and H. Q. Luo, *ACS Appl. Mater. Interfaces*, 2016, **8**, 21700–21709.
27 S. K. Makkad and S. K. Asha, *ACS Biomater. Sci. Eng.*, 2017, **3**, 1788–1798.
28 S. K. Makkad and S. K. Asha, *Anal. Chem.*, 2018, **90**, 7434–7441.
29 J. R. Lakowicz, *Principles of Fluorescence Spectroscopy*, Springer: New York, 3rd edn, 2006, DOI: 10.1007/978-0-387-46312-4.

 This journal is © The Royal Society of Chemistry 2020